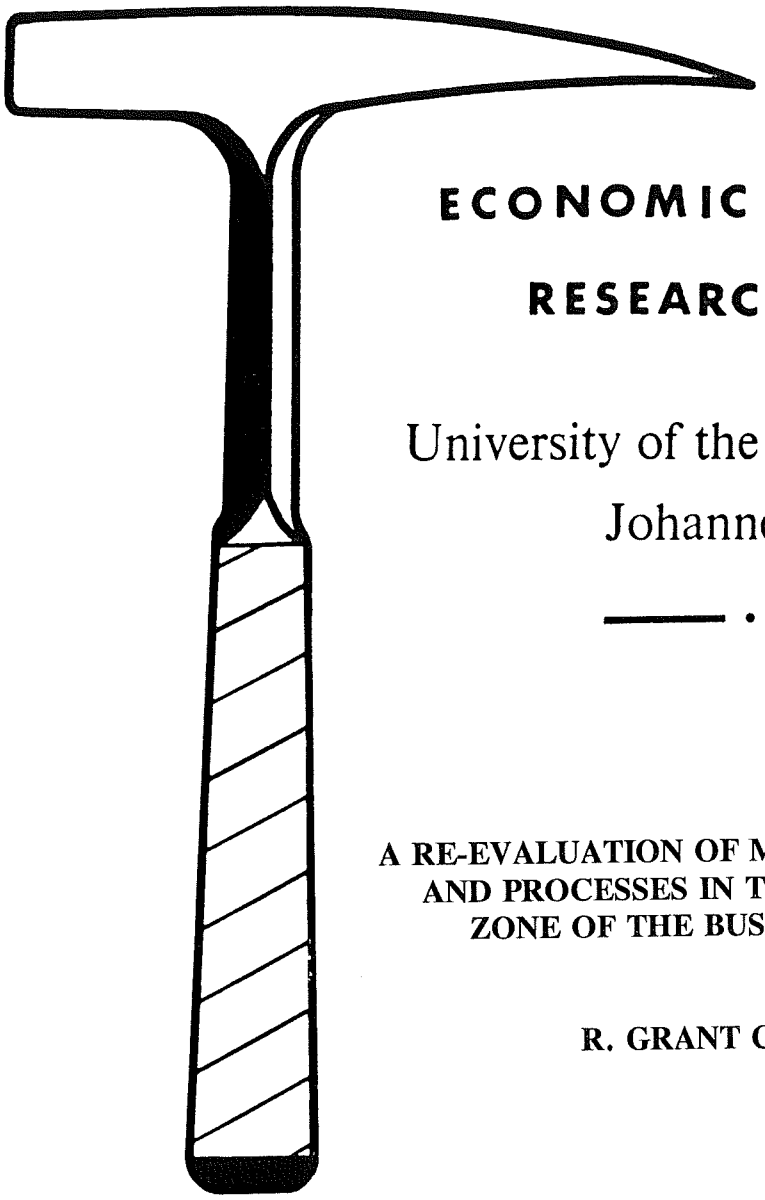

ECONOMIC GEOLOGY
RESEARCH UNIT

University of the Witwatersrand
Johannesburg

A RE-EVALUATION OF MAGMA COMPOSITIONS AND PROCESSES IN THE UPPER CRITICAL ZONE OF THE BUSHVELD COMPLEX

R. GRANT CAWTHORN

INFORMATION CIRCULAR No. 286

UNIVERSITY OF THE WITWATERSRAND
JOHANNESBURG

A RE-EVALUATION OF MAGMA COMPOSITIONS AND PROCESSES IN THE UPPER CRITICAL ZONE OF THE BUSHVELD COMPLEX

by

R. GRANT CAWTHORN
(Department of Geology, University of the Witwatersrand, P/Bag 3, WITS 2050, Republic of South Africa)

ECONOMIC GEOLOGY RESEARCH UNIT
INFORMATION CIRCULAR No. 286

February, 1995

A RE-EVALUATION OF MAGMA COMPOSITIONS AND PROCESSES IN THE UPPER CRITICAL ZONE OF THE BUSHVELD COMPLEX

ABSTRACT

A detailed geochemical study is presented of the uppermost Critical Zone, especially of the footwall to the Merensky Reef at Impala Platinum Mines. The approximately 100m-thick sequence below the Merensky Reef consists of 13 distinct units which have sharp boundaries. They are adcumulates with varying proportions of plagioclase and orthopyroxene, and are devoid of any other cumulus minerals.

Information on the En content of orthopyroxene and *mg#* (100*Mg/Mg+Fe) number of whole rocks can be combined with experimental studies to indicate that the magma producing the footwall sequence contained $\pm$ 5% MgO. The magma to the Merensky Reef was not ultrabasic, but contained $\pm$ 4% MgO, and was *more evolved* than the footwall magma.

Significant variations exist for both the En content of orthopyroxene and *mg#* number of whole rocks in short vertical sections. Pyroxenite and norite always have higher values than anorthosite. Extremely sharp breaks in these values occur, corresponding with changes in modal proportion, and argue against both fractional crystallization and significant infiltration metasomatism. Quantitative modelling shows that the entire footwall section could have contained pyroxene with a uniform primary composition of En_{83}, and that all the variation now observed reflects the effect of reaction with *trapped* magma.

Two independent methods for determining the proportion of trapped magma are presented, based on *mg#* number and incompatible element abundances. Both yield a uniform and low proportion in all samples of approximately 10%.

Immiscible sulphide liquid from the Merensky Reef can be shown to have infiltrated downwards for no more than 4m, despite its high density contrast with silicate magma, very low viscosity and low crystallization temperature. The footwall, 5m below the magma-cumulate interface, is shown to be impermeable even to sulphide liquid. Residual silicate magma would be even more restricted in its mobility.

The fluxing of residual magma through pothole structures in the floor of the Merensky Reef is not supported by the present data.

_____oOo_____

A RE-EVALUATION OF MAGMA COMPOSITIONS AND PROCESSES IN THE UPPER CRITICAL ZONE OF THE BUSHVELD COMPLEX

CONTENTS

_____oOo_____

Published by the Economic Geology Research Unit
Department of Geology
University of the Witwatersrand
1 Jan Smuts Avenue
Johannesburg 2001
South Africa

ISBN 1 86838 154 4

A RE-EVALUATION OF MAGMA COMPOSITIONS AND PROCESSES IN THE UPPER CRITICAL ZONE OF THE BUSHVELD COMPLEX

INTRODUCTION

The fate of interstitial magma in a slowly cooled layered intrusion is potentially important. Migration of residual magma could alter mineral compositions, change the final mineralogy, or even produce major mineral deposits, such as the platinum-rich Merensky Reef (Boudreau and McCallum, 1992). In the concepts summarized by Wager *et al.* (1960) this magma was assumed to have remained stagnant and frozen *in situ* to produce a variety of interstitial phases and zoned overgrowths on existing minerals. Barnes (1986a) presented quantitative modelling of this principle to show how mafic phases, such as olivine and pyroxene, rapidly re-equilibrate with magma to produce internally homogeneous grains, and can change their composition by an amount proportional to both the fraction of trapped liquid and the modal proportion of that phase. This was referred to as the trapped liquid shift effect. However, it was also recognised that deformation and compaction could cause migration of that liquid (McKenzie, 1984). Even small proportions of magma could be squeezed out, provided the time scale is long enough, although this may not be the case in crustal reservoirs. The subsequent reaction of this magma with minerals with which it was not originally in equilibrium was termed infiltration metasomatism by Irvine (1980). A comparison of the relative densities of magmas produced as a result of the crystallization of various assemblages led to the recognition that dense magma could sink within the crystal pile and drive a process described as compositional convection (Tait *et al.*, 1984). Such processes were seen as being pervasive, but it is also possible that they could become channelized. This would decrease the ratio of primary assemblage to transgressing magma, permitting more extensive reaction, ultimately resulting in replacement of some or all of the original mineralogy. Discordant "finger" structures and larger "chimneys" have been interpreted in this way (Robins, 1982; Tait and Jaupart, 1992).

This study focuses on a short vertical section through the upper Critical Zone of the Bushveld Complex, to examine geochemical evidence which throws light on the relative importance of migration versus trapping of residual magma.

GEOLOGICAL SETTING

The upper Critical Zone of the Bushveld Complex has been the subject of numerous studies, because of the presence of the platinum-rich Merensky Reef and also because it contains some spectacular mineral layering with rocks containing every possible proportion of pyroxene, plagioclase and chromite. Many of these studies have made use of borehole core and underground access associated with mining in the western Bushveld Complex (Fig. 1).

Within the upper Critical Zone a gross cyclicity has been recognised, on a scale from 10 to 100m, consisting of a basal chromite-rich layer followed by pyroxenite (which may occasionally contain olivine), norite and anorthosite. At least seven such cycles exist. Part of this section from Impala Platinum Mines is shown in Figure 2, where the Merensky Reef cyclic unit is some 15m thick, and the underlying cycle, referred to as the Upper Group 2 Chromitite cycle (UG2) is over 100m thick (Leeb-du Toit, 1986). It was shown by Eales

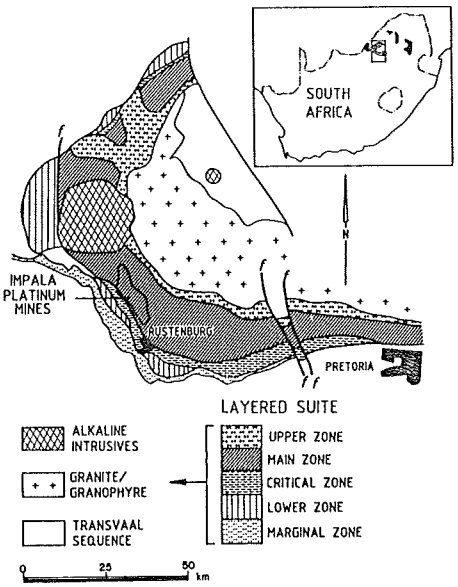

Figure 1: Simplified geological map of the western Bushveld Complex showing the location of Impala Platinum Mines.

et al. (1986) that each cycle had a slightly different ratio of Sr/A1, and they argued that this was evidence that each cycle was initiated by addition of chemically distinct magma. This conclusion was also reached by Naldrett *et al.* (1986) on the basis of reversals in the *mg#* or 100*Mg/(Mg+Fe) ratio of orthopyroxene. This interval, from the UG2 Chromitite layer to the top of the Critical Zone on Impala Platinum Mines, has been investigated by Schurmann (1993) who refined the above models and proposed the emplacement of numerous minor injections of magma of different compositions into a stratified chamber on the basis of variations in mineral compositions.

The actual lithological variation within a cycle is in fact more complicated than simply chromitite, pyroxenite, norite, followed by anorthosite, as shown in Figure 2, and a total of 13 continuous layers can be identified in the UG2 cycle (Leeb-du Toit, 1986). At the base is a 6m-thick pyroxenite, followed by a complex sequence of norite, leuconorite and anorthosite. Contacts are sharp to gradational over a few centimetres between all units. Most units are relatively homogeneous internally although some modal variation does occur. For example, in the 5 m-thick footwall 3 (F3) there is a gradual upwards increase in pyroxene content (Cawthorn and Poulton, 1988).

In this study, samples were taken from ten boreholes, from the top of the Merensky cyclic unit (M3) down to footwall 6 (F6). Considerable modal variation occurs within this +/- 40 metre-thick interval, whereas below this lies a very thick (over 40 m) homogeneous norite (F7). Samples have been collected at approximately 1 m intervals. The stratigraphic and petrographic details of this package have been documented elsewhere (Leeb-du Toit, 1986; Schurmann, 1993) and will not be repeated here. It is sufficient to note here that the

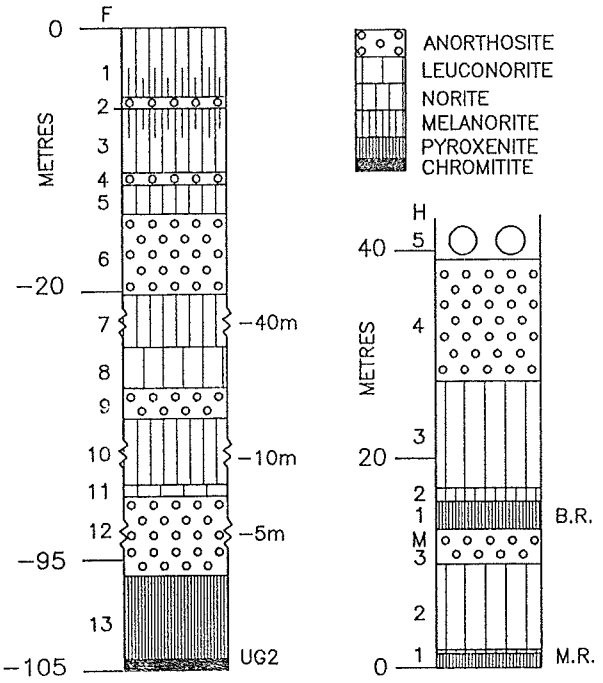

Figure 2: Schematic section through the uppermost Critical Zone on Impala Platinum Mines. F, M and H refer to footwall, Merensky and hanging wall cyclic units respectively, using the scheme of Leeb-du Toit (1986). UG2, M.R. and B.R. refer to Upper Group 2 Chromitite layer, Merensky and Bastard Reefs. Depths in metres refers to depths relative to the Merensky Reef. Note that three intervals (of 40, 10 and 5m) of thick homogeneous sequences have been excluded from the lower succession.

the silicate rocks can be classified as adcumulates, consisting of varying proportions of plagioclase and orthopyroxene, with never more than trace contents of chromite, clinopyroxene and biotite. The other feature of importance is the presence of potholes in the base of the Merensky Reef. These are roughly circular features in plan and of variable diameter, which erode the footwall stratigraphy to variable depths. On Impala Platinum Mines, however, they frequently bottom against the footwall 3 unit (Leeb-du Toit, 1986).

GEOCHEMISTRY

All samples have been analyzed by XRF spectrometry for major and trace elements, and a representative suite from one borehole core is presented in Table 1. As they are almost pure adcumulates containing variable proportions of two minerals, their major element compositions reflect this, and all binary plots demonstrate a constrained linear trend between the compositions of plagioclase and orthopyroxene (Fig. 3).

The adcumulate nature of these rocks is demonstrated by the low concentrations of

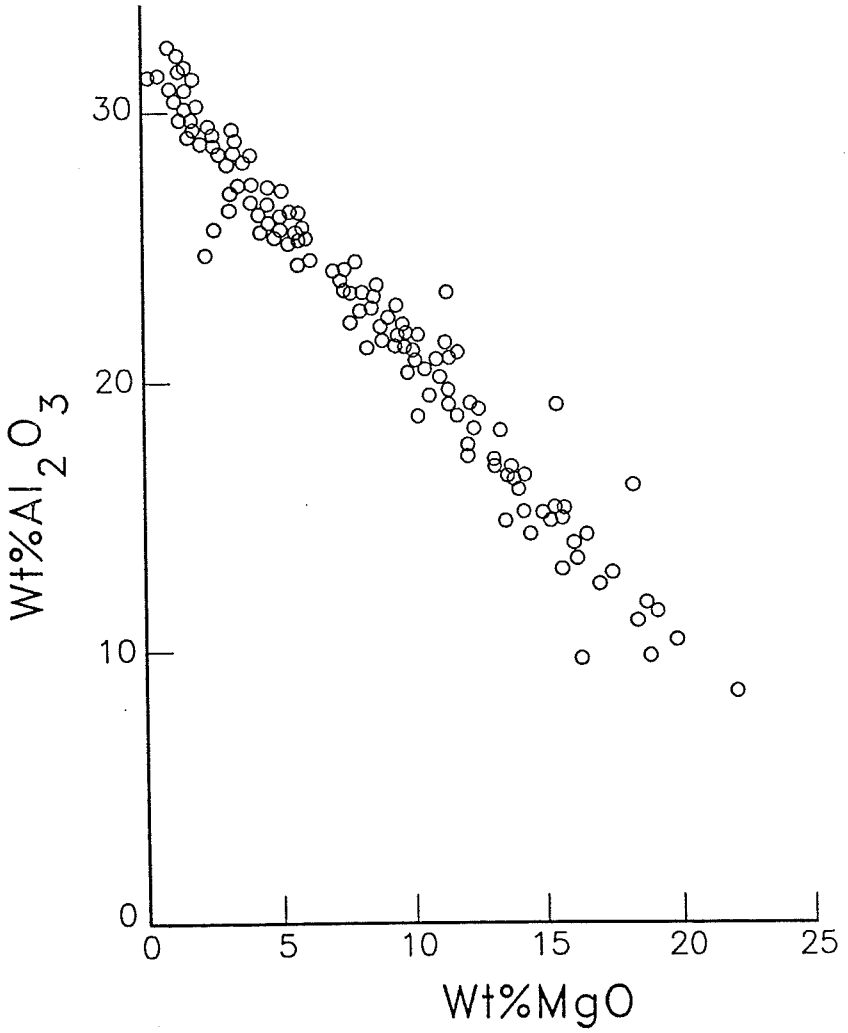

Figure 3: Plot of whole-rock MgO versus Al_2O_3 for 180 samples. Many samples with less than 10 wt % MgO are not ploted because of the density of points. This plot demonstrates that the samples represent mixing between plagioclase and orthopyroxene.

incompatible elements, such as K_2O, P_2O_5, Rb, Zr, Y and Nb (Table 1). The range of concentrations of these elements is quite restricted as shown by a histogram of Zr abundances in Figure 4. Very few samples plot outside the range of 15 to 25 ppm Zr, suggesting a remarkably uniform intercumulus component. Furthermore, there does not appear to be any significant difference between samples above and below the Merensky Reef.

The variation in composition with height is illustrated in Figure 5A, showing the MgO content through one vertical section. The abruptness of the modal layering can be seen by the sudden changes in MgO across boundaries, such as between footwall 6 and 5. In footwall 3 the upwards increase in MgO, which reflects pyroxene content, can be seen. Individual mineral analyses have not been undertaken on all these samples. However, as orthopyroxene is the only mafic phase present the *mg#* of the whole rock and the orthopyroxene will be identical. Hence, the plot of *mg#* versus height, shown in Figure 5B, essentially illustrates

Table 1: Representative whole-rock chemistry of samples from one borehole

Depth*	6.58	5.73	4.31	2.69	1.24	-.36	-.61	-1.46	-3.96	-4.86	-5.16	-5.36	-7.06
Unit	M2	M2	M2	M2	M2	F1	F1	F1	F1	F1	F2	F3	F3
SiO2	50.10	50.24	50.95	50.70	52.43	49.59	49.99	49.22	50.34	51.65	51.57	51.89	51.36
TiO2	.08	.10	.13	.10	.19	.09	.09	.09	.09	.14	.10	.15	.12
Al2O3	29.68	27.75	25.14	25.26	12.49	25.13	23.55	23.38	23.61	14.47	22.41	15.45	21.46
Fe2O3	2.14	3.14	4.03	4.09	9.69	4.21	4.61	3.83	4.26	7.56	4.02	7.73	5.18
MnO	.05	.05	.08	.09	.17	.07	.06	.09	.10	.17	.10	.14	.10
MgO	2.16	3.90	5.66	5.86	17	6.26	8.07	7.51	7.86	16.59	9.11	15.83	9.90
CaO	14.65	13.94	13.09	12.73	7.53	12.55	11.80	11.87	12.11	7.92	11.88	8.28	11
Na2O	2.05	2.25	1.81	1.89	1.18	1.80	2.15	1.78	1.72	1.15	1.67	1.20	1.54
K2O	.20	.19	.18	.17	.12	.18	.16	.15	.15	.11	.18	.15	.16
P2O5	.02	.03	.03	.03	.02	.02	.03	.02	.02	.02	.02	.02	.03
LOI	.24	.13	.10	.08	-.08	.31	.38	3.17	.38	.15	.30	.16	.45
Total	101.37	101.72	101.20	101.00	100.74	100.21	100.89	101.11	100.64	99.93	101.36	101.00	101.30
Cu	47	44	51	72	293	861	471	18	16	27	16	18	7
Ni	95	116	153	201	26	1616	1040	140	141	381	177	393	225
Rb	3	4	5	4	4	2	4	2	3	4	3	5	3
Sr	359	334	310	318	173	340	329	339	319	206	301	228	276
Zr	20	22	23	19	22	18	21	19	16	21	19	21	20
Y	3	4	4	4	8	3	6	4	6	7	5	5	6
V	31	44	57	51	118	41	49	48	48	82	60	81	60
Cr	159	383	562	552	1936	638	921	913	974	2077	1161	1780	1219
mg#	66.7	71.1	73.6	73.9	77.7	74.6	77.6	79.5	78.5	81.3	81.8	80.2	79.1
IL(Zr)**	13	15	15	13	15	12	14	13	11	14	13	14	13
IL(K)**	13	13	12	11	8	12	11	10	10	7	12	10	11

Depth*	-8.26	-9.16	-9.76	-10.41	-10.90	-11.16	-12.04	-13.34	-14.22	-15.26	-16.35	-17.90	-18.57
Unit	F3	F3	F3	F5	F5	F6	F6	F6	F6	F6	F6	F6	F6
SiO2	51.32	51.73	50.46	50.93	51.07	48.95	48.44	49.34	49.72	49.26	49.41	49.67	50.45
TiO2	.13	.12	.09	.13	.13	.05	.06	.07	.06	.05	.05	.06	.08
Al2O3	20.83	22.62	25.65	18.42	21.62	30.90	29.65	27.14	29.55	31.16	32.49	31.52	22.96
Fe2O3	5.33	4.60	3.36	6.82	5.50	1.31	1.48	3.27	1.49	1.17	.41	.75	4.10
MnO	.10	.11	.08	.15	.12	.05	.03	.06	.04	.02	.02	.03	.07
MgO	10.40	9.33	5.59	12.30	9.81	1.52	2.21	4.99	1.97	1.97	.95	1.59	9.18
CaO	10.55	11.30	13.32	9.46	11.15	15.27	14.47	13.58	14.93	15.19	15.47	15.55	11.25
Na2O	1.58	1.63	1.91	1.39	1.59	2.55	2.05	1.86	2	2	2.12	2.07	1.48
K2O	.16	.14	.17	.12	.17	.15	.25	.11	.15	.12	.17	.13	.10
P2O5	.02	.03	.02	.02	.02	.02	.03	.02	.03	.02	.02	.02	.01
LOI	.04	-.03	.24	.56	.14	.28	1.20	.12	.06	.15	.40	.21	.53
Total	100.46	101.58	100.89	100.30	101.32	101.05	99.87	100.56	100.00	101.11	101.51	101.60	100.21
Cu	9	13	14	55	8	5	6	8	6	2	2	3	3
Ni	267	261	139	465	225	24	31	69	0	0	0	0	128
Rb	3	3	4	3	6	2	5	4	6	5	7	7	6
Sr	296	302	352	241	278	424	429	408	364	373	401	403	289
Zr	24	21	17	20	23	16	16	16	13	14	14	15	17
Y	4	3	4	2	3	3	3	2	7	4	7	6	8
V	61	56	45	70	62	26	19	28	28	19	16	11	58
Cr	1208	1055	750	1552	1295	445	107	439	641	238	134	10	1080
mg#	79.4	82.9	76.7	78.1	78.1	69.7	74.7	74.7	75.1	75.1	76.9	82.1	81.6
IL(Zr)**	16	14	11	13	15	11	11	11	9	9	9	10	11
IL(K)**	11	9	11	8	11	10	17	17	7	10	8	11	7

*Depth refers to depth in metres relative to the base of the Merensky Reef
**IL refers to per centage of interstitial liquid using Zr and K2O contents

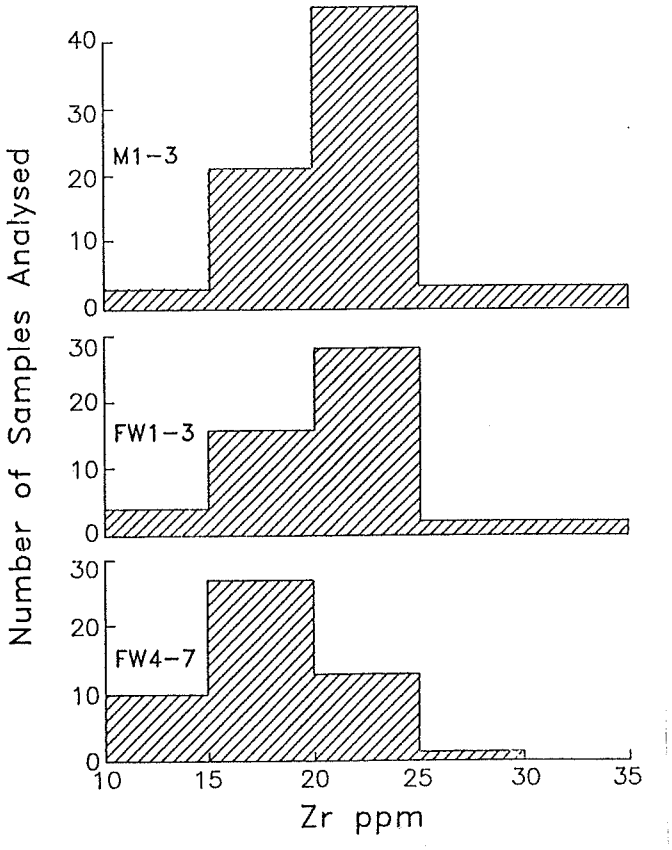

Figure 4: Histogram plot of Zr abundances in all samples, divided into three stratigraphic units, those above the Merensky Reef (M1-3), those in the immediate footwall (F1-3), and those in the deeper footwall (F4-7).

the changes in orthopyroxene composition through this interval. In the anorthositic footwall 6 the *mg#* is much lower than in the associated more mafic rocks.

INTERPRETATION

Several aspects relating to the evolution of this sequence of rocks can be evaluated from this data base. These include:

1. the role of fluid, channelled through pothole structures;
2. addition of magma and its contribution to cyclic layering;
3. the composition of this magma;
4. migration of residual magma within the cumulate pile; and
5. the proportion of interstitial component.

Fluids and Pothole Structures

It has been suggested that potholes are the site of fumarolic activity or migration of residual fluids (Boudreau, 1992). Based on a study of three pairs of borehole intersections

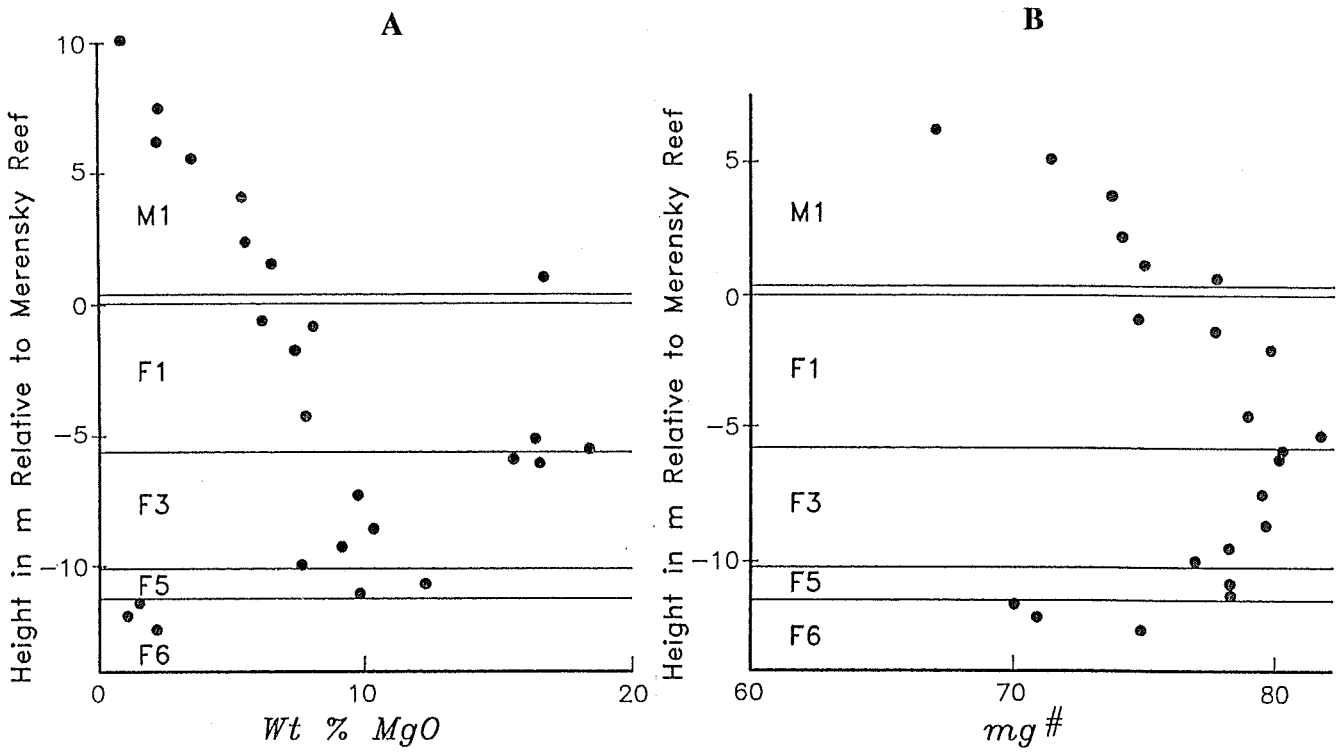

*Figure 5: Plot against height relative to the Merensky Reef of whole-rock MgO (Fig. 5A) and mg# defined as 100*Mg/(Mg+Fe) (Fig. 5B).*

through the immediate footwall to potholes and unpotholed Merensky Reef, Cawthorn and Poulton (1988) suggested that there was enrichment in mobile, incompatible elements under potholes, consistent with this hypothesis. They showed that K_2O, Rb and Cu were enriched in footwall 3 below potholes in two of the three profiles studied relative to adjacent unpotholed footwall 3. No enrichment in immobile, incompatible elements, such as TiO_2 and P_2O_5, was noted, and so the increase in the mobile incompatible elements was not attributable to a greater proportion of residual liquid. In this study a further three pairs of boreholes have been analyzed. The sequence immediately above the Merensky Reef was also analyzed in this study as the intention was to determine if such fluids could be recognised traversing post-Merensky layers, or whether they terminated at the Merensky Reef. Such information would have indicated the relative timing of migration of such fluids. The results are presented in a histogram of K_2O contents in Fig. 6. The 48 samples from the immediate footwall (F1 to F3) to potholed Reef show lower K_2O contents than the 72 samples from footwall to normal Reef. Of the total data base from this and the study of Cawthorn and Poulton (1988), only two of the six borehole intersections through potholed reef show enriched incompatible element abundances; and so the conclusion of Cawthorn and Poulton (1988) has not been substantiated by this study. Samples from the Merensky cyclic unit show no difference in abundance between potholed and unpotholed intersections, and also contain the same average K_2O content as the footwall.

The higher Cu values reported by Cawthorn and Poulton (1988) in the footwall to potholed environments will be discussed below.

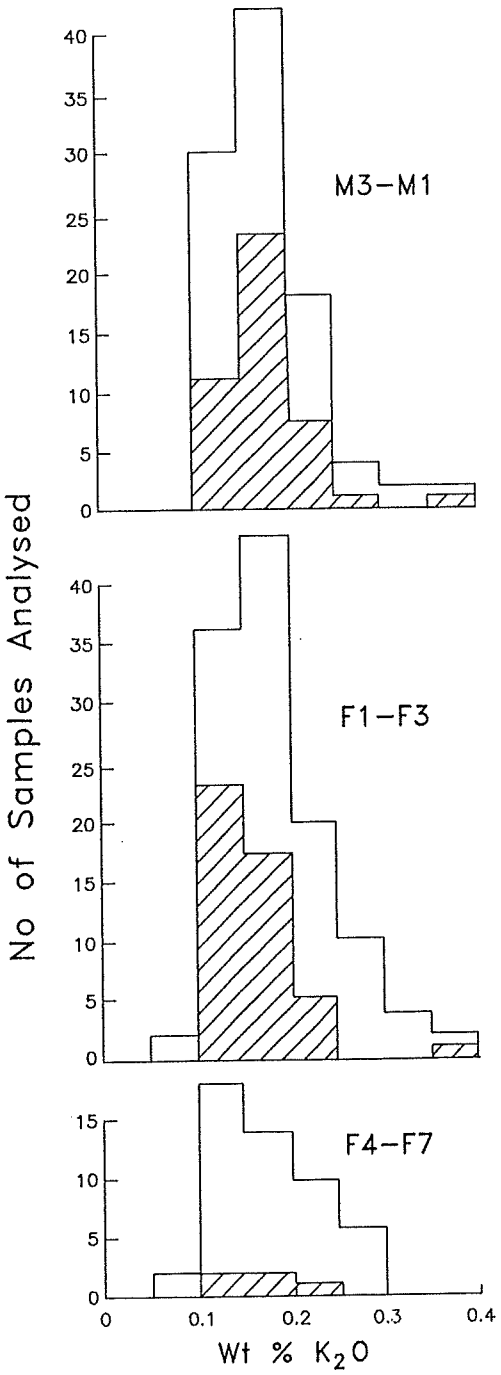

Figure 6: Histogram of K_2O contents in in the Merensky Reef cyclic unit (M1 to M3), immediate footwall (F1 to F3) and deep footwall (F4 to F7). Shaded samples are from bore core intersecting potholed Merensky Reef; unshaded from normal Reef Sections

Magma Addition

Eales *et al.* (1988) used the existence of distinct breaks in the ratio of Sr/Al_2O_3 in vertical sections to argue for addition of magma of different composition. Such a break at the level of the Merensky Reef is supported by the trends displayed on a plot of MgO versus Sr presented in Figure 7. This is analogous to the MgO versus Al_2O_3 in Figure 5, which

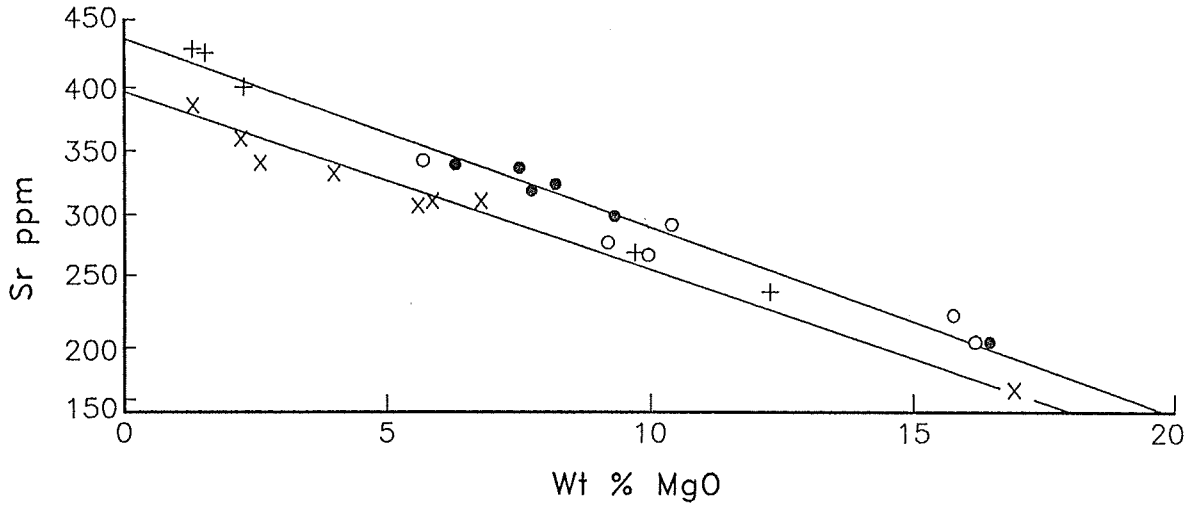

Figure 7: Plot of whole-rock MgO versus Sr for samples from one borehole. Samples from the Merensky cyclic unit are designated with a cross. Solid dots, open dots and plus symbols refer to samples from footwalls 1 and 2; 3 and 4, 5 and 6, respectively. The upper and lower lines define trends for samples below and above the Merensky Reef respectively.

shows a linear mixing trend between plagioclase and orthopyroxene. However, this diagram shows clearly that samples from above the Merensky Reef define a trend with a lower Sr content than samples from below the Reef, consistent with the conclusion of Eales *et al.* (1988) that the sequence from above the Merensky Reef formed from a magma with a different Sr content. The colinearity of all the samples from the footwall implies formation from a magma of constant composition.

Composition of the Magma

The nature of the compositions of the resident and any added magmas forming the upper Critical Zone has been extensively debated, as it has bearing on mechanisms for the formation of Merensky Reef-type mineralization. Irvine *et al.* (1983) suggested that two fundamentally different, and unrelated, magmas were interstratified within the chamber, one being ultrabasic, the other being anorthositic. Each formed its own characteristic cumulates (pyroxenite and anorthosite respectively), while mixing between them resulted in chromitite and sulphide formation. Naldrett *et al.* (1986) suggested that the magma that was intruded at the level of the Merensky Reef was ultrabasic and that the immediate footwall had formed from an extensively differentiated magma of the same original composition. Eales *et al.* (1993) envisaged a similar process, although recognising that a distinct break in the initial $^{87}Sr/^{86}Sr$ ratio at the level of the Merensky Reef required a magma with a different history from the previous injections. In all these studies the UG2 (Upper Group 2 Chromititie) cyclic unit comprising the footwall to the Merensky Reef was regarded as having been derived from a single magma, whereas Schurmann (1993) envisaged the involvement of six injections of a suite of magmas related to those proposed by Harmer and Sharpe (1985) to produce the

sequence from footwall 13 to footwall 1 in Figure 2.

As these rocks are cumulates, formed after the possible mixing in various proportions of different magmas, it is impossible to determine uniquely the composition of either resident or injected magma. However, it is possible to constrain the MgO content of the magmas using the composition of orthopyroxene. In the entire interval from the UG2 chromitite to the Merensky Reef the most magnesian orthopyroxene has an *mg#* of 83 (according to Naldrett *et al.*, 1986; Eales *et al.*, 1993; Schurmann, 1993). In the more leucocratic rocks *mg#* decreases to less than 70.

It is generally accepted that these pyroxenes have formed at some stage of differentiation of magma whose composition was identified by Cawthorn and Davies (1983) as containing ± 13% MgO. Subsequent studies on this composition by Barnes (1986b) and Cawthorn and Biggar (1993) yielded compositions of coexisting orthopyroxene and silicate liquid. The relevant results are summarized in Table 2 and Figure 8. These show that orthopyroxene of composition En_{90} crystallizes from a magma with 11% MgO at about 1300°C. The magma in equilibrium with En_{83} only contains 5 to 6% MgO. Thus the magma from which the pyroxenite of the upper Critical Zone formed is far from being ultrabasic. Experimental data show that such a magma will also be saturated with plagioclase, a conclusion presented by Eales *et al.* (1993) using trace element contents of orthopyroxene.

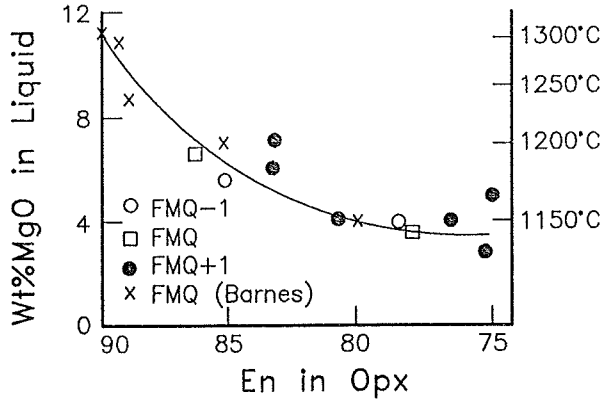

Figure 8: Compositions of orthopyroxene and co-existing silicate liquid obtained from experimental studies at various oxygen fugacity on probable parental magma to the Bushveld Complex, based on analyses from Barnes (1986b, denoted by cross) and Cawthorn and Biggar (1993). An approximate temperature is also indicated.

Migration of Residual Magma

Reaction between primary orthopyroxene and trapped residual liquid causes the En content to decrease. If there has been migration of such liquid across a boundary where a reversal in composition has taken place then pyroxene occurring above such a reversal would have its En content decreased by reaction with highly differentiated liquid (Irvine, 1980). Thus total variations in primary En content within a short vertical interval could have been reduced by such processes.

Table 2: Co-existing pyroxene and liquid compositions

A.							
Temp °C	1283	1281	1205	1184	1184	1139	1139
Buffer*	fmq-1	fmq+1	fmq	fmq-1	fmq+1	fmq-1	fmq+1
Liquid compositions							
SiO2	56.65	57.26	57.43	58.46	57.01	61.53	59.32
TiO2	.39	.38	.44	.45	.45	.90	.91
Al2O3	12.52	12.46	14.20	14.59	14.75	14.65	13.16
FeO	7.52	8.20	7.67	6.68	7.64	6.32	7.18
MnO	.17	.17	.15	.14	.14	.09	.11
MgO	8.40	9.42	6.44	5.24	5.74	2.92	3.99
CaO	6.91	6.72	7.84	7.92	7.92	6.06	7.01
Na2O	2.90	2.49	2.54	2.72	2.68	2.42	1.75
K2O	2.79	2.17	1.81	2.36	1.98	3.23	2.16
P2O5	.25	.29	.24	.31	.35	.41	.30
Cr2O3	.11	.07	.04	.05	.08	.03	.02
Total	98.61	99.63	98.80	98.92	98.74	98.56	95.90
Phase	Ol	Ol	Opx	Opx	Opx	Opx	Opx
SiO2	39.75	40.50	55.91	53.25	56.03	54.81	54.28
TiO2			.07	.09	.10	.10	.10
Al2O3	.05	.10	1.30	1.45	.88	.80	.95
Cr2O3	.11	.10	.34	.69	.22	.09	.17
FeO	12.07	9.60	8.95	15.79	9.72	15.23	14.31
MnO	.23	.19	.20	.24	.24	.30	.30
MgO	47.05	49.65	31.85	26.64	31.52	27.80	29.35
CaO	.30	.21	1.37	.90	1.18	.80	.90
Total	99.56	100.35	99.99	99.05	99.89	99.93	100.36
mg#	87.42	90.21	86.38	75.04	85.25	76.49	78.52

B.						
Temp °C	1334	1299	1264	1254	1209	1158
Buffer*	fmq	fmq	fmq	fmq	fmq	fmq
MgO(L)	13.51	11.17	10.99	8.76	7.29	4.01
FeO(L)	9.15	7.93	8.54	7.33	8.23	7.86
mg#(Opx)	90.40	90.85	89.70	89.04	86.65	80.20

A. Previously unpublished analyses from experimental study of Cawthorn and Biggar (1993).
B. Summary of MgO and FeO contents of liquids and mg# in orthopyroxene from study of Barnes (1986b).

Buffer* - fO_2 relative to fayalite-magnetite-quartz buffer

The pyroxene compositions from the UG2 chromitite to the top of the Merensky cyclic unit are shown in Figure 9. Two apparent differentiation sequences with an intervening reversal might be inferred from these values. Between the top of the footwall and the base of the Merensky Reef there is a change in En content from 68 to 81 over a vertical interval of 2m in the Union Mine profile, from 77 to 83 in the Rustenburg Mine profile, and from 76 to 79 (for whole-rock *mg#*) in the Impala Platinum Mines profile (Fig. 5B). Had there been significant upward migration of residual liquid from footwall cumulates into the Merensky Reef such sharp breaks would not have been preserved. Furthermore, the lowermost cumulates of the Merensky Reef would show an upward increase in En content concomitant with the diminishing influence of upward-migrating liquid, as in the infiltration metasomatism model of Irvine (1980). Downward migration of dense residual magma from the Merensky Reef into the footwall would have caused an increase in En values in pyroxene in the immediate footwall. Neither trend is observed. Thus, these data argue against migration of residual magma.

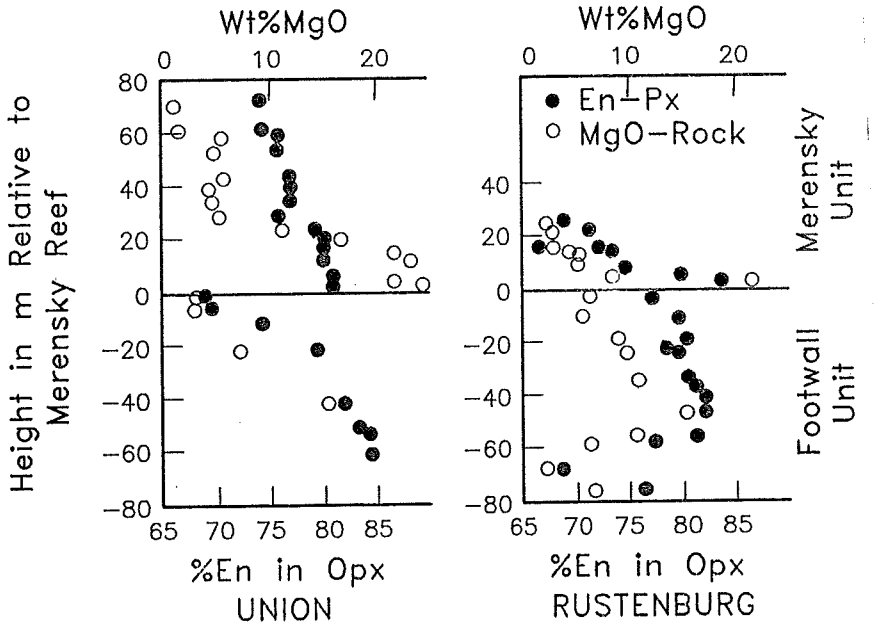

Figure 9: Plot of En content of orthopyroxene (solid dots) and MgO content of whole rock samples (open dots) as a function of height relative to the Merensky Reef in the upper Critical Zone for two profiles some 70 km apart (taken from the study of Naldrett et al., 1986).

The data of Naldrett *et al.* (1986) and those presented here can be treated quantitatively to examine the influence of residual magma. Naldrett *et al.* (1986) attributed the trends shown in Figure 9 to fractional crystallization, with the cycle from the top of the UG2 to the base of the Merensky Reef behaving as a single homogeneous magma. This conclusion ignored the fact that the An content of the plagioclase actually increased upwards, through this same section.

A detailed study of one unit within the UG2 cycle, the noritic footwall 7, shows that the En content of the pyroxene remains absolutely constant for over 40 m (Figure 10). In contrast, the more detailed study of footwall 1 to 6, shown in Figure 5, indicates that there are reversals in the *mg#* within this cycle. Also, footwall 3 shows an upwards increase in the *mg#* content as the unit becomes more mafic. In yet another, even more detailed section, it can be seen (Fig. 11) that there are sudden dramatic decreases in the *mg#*. For example, at the contact between the noritic footwall 7 and the anorthositic footwall 6 the *mg#* decreases from a uniform value of 81 to less than 60 within 30 cm. A similar decrease is seen at the base of footwall 4. Thus, an examination of the details within this cyclic unit reveals that whereas there appears to be an overall upward differentiation in terms of En content of the pyroxene, there are considerable thicknesses which show no differentiation; others which show abrupt reversals; and yet others with extremely sharp forward displacements in the differentiation index. Such observations would seem to require extremely complicated processes occurring within the magma.

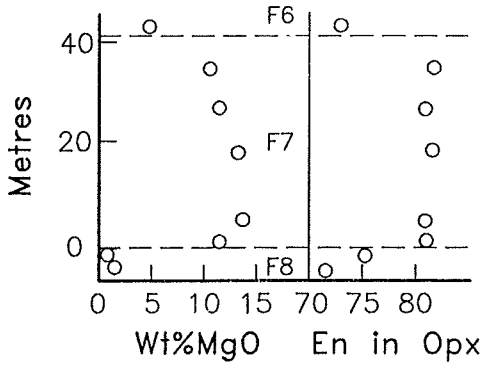

Figure 10: Plot of whole-rock content and En content of orthopyroxene versus vertical height in footwall unit 8 and its adjacent units (from Schurmann, 1993). The pyroxene is of uniform composition throughout the entire 40m of the noritic footwall 7, but is distinctly depleted in En in the over- and underlying anorthositic layers.

Reference to Figs 5, 9 and 10 shows that there is an extremely good correlation between En in orthopyroxene or *mg#* of the whole rock and the MgO content of the whole rock. Given the complex vertical variations in modal proportion of plagioclase to pyroxene shown in Fig. 2, this is difficult to explain in terms of fractionation from a single magma. The models of Naldrett *et al.* (1986) and Schurmann (1993) assume that the composition of the pyroxene is that of the primary mineral. If there is reaction between primary phase and residual liquid this need not necessarily be correct. In the extreme case where the primary minerals trap the residual liquid from which they formed, Barnes (1986a) showed that the extent of change of the mineral composition varied with the relative proportions of the primary phase and trapped liquid, and in the case of pyroxene the MgO and FeO content of the trapped liquid. If this has been a significant process in controlling the composition of the pyroxene the biggest shift in the En content of the pyroxene should occur in the anorthositic (low MgO) rocks, as is observed; and as was first reported by Ferguson (1969).

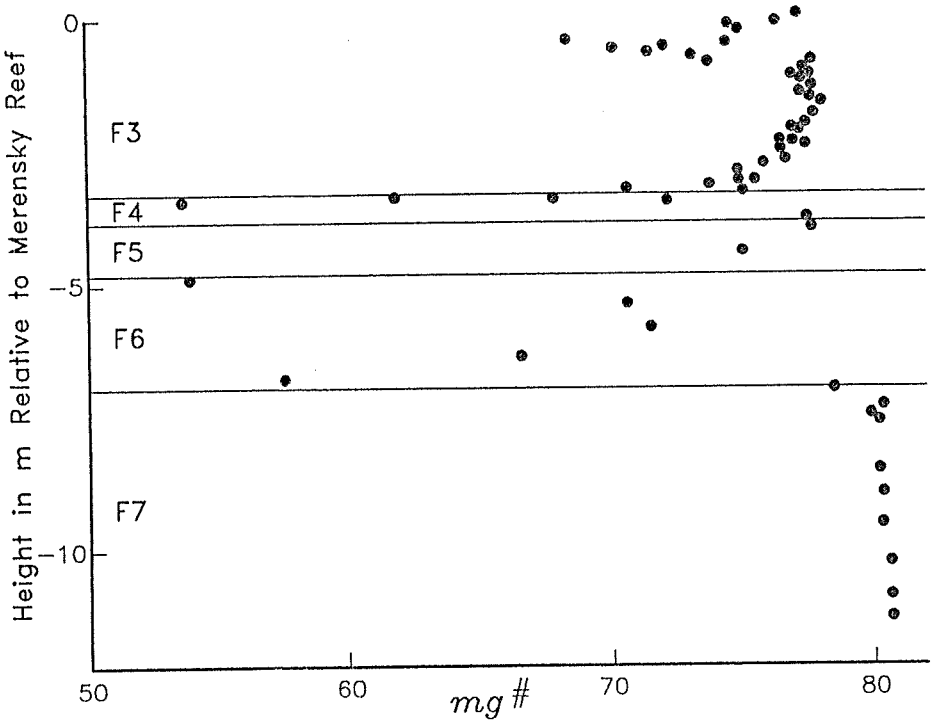

Figure 11: Plot of whole-rock mg# versus height in footwall units 3 to 7, sampled at 20cm spacing. There are extremely sudden breaks in mg# between adjacent units.

In all of these diagrams and interpretations it has been assumed that there has been absolutely no vertical migration of magma. This can be confirmed from this data set. In Fig. 11 the whole-rock *mg#* decreases from 81 to less than 60 over a vertical interval of 20 cm, in moving from a norite to an anorthosite. If residual liquid had migrated upwards, the lowest sample immediately above this sharp break would have been infiltrated by magma with a high *mg#* value and would therefore have been reset to higher values. As this rock is an anorthosite with very little pyroxene such resetting would have been easily accomplished. The preservation of such a sharp break at the boundary clearly demonstrates that no residual magma migrated upwards.

Evaluating the possibility of downward migration of residual magma can be attempted using the data and that of Kruger and Marsh (1982) and Eales *et al.* (1986). Kruger and Marsh (1982) used the initial Sr isotopic ratio to demonstrate that the Merensky Reef had formed from a magma isotopically distinct from its footwall. The sudden increase in this ratio occurred at and immediately above the base of the Reef. There is no evidence in their data, even for samples less than 1m below the Reef, that the ratio began to increase below the Reef as would be expected if downward infiltration of a magma with a higher ratio had occurred. The same argument can be used for the Sr/Al ratio plot of Eales *et al.* (1986) where sharp breaks occur at the bases of all five cyclic units studied.

Composition of Parental Magma and Cumulus Pyroxene

Exact calculations of the trapped liquid shift effect on pyroxene compositions for the present suite of rocks are simple as the system involves plagioclase with zero MgO and FeO, pyroxene and liquid. Furthermore, the MgO and FeO contents of the liquid have been constrained from experimental studies mentioned above (Table 2). It is therefore possible to calculate any bulk-rock MgO and FeO content assuming varying proportions of plagioclase, pyroxene and magma. An example of this calculation is shown in Table 3, and modelled curves are shown in Figure 12. Trapped liquid proportions of 10 and 30% are used in these calculations. If there is only 10% trapped liquid (curves A to C; Fig. 12), then the *mg#* for the bulk rock changes very little as the proportion of primary pyroxene changes from 90 to 30% (equivalent to 30 to 10% whole-rock MgO). However, at lower proportions of primary pyroxene major shifts in *mg#* are predicted. The curve for 30% trapped liquid displays a more gradual change in the whole-rock *mg#*.

Table 3

TRAPPED LIQUID SHIFT EFFECT ON PROPORTIONS AND COMPOSITIONS OF PYROXENES

	Primary Opx	Magma	90%Opx + 10%Magma	40%Opx + 50%Plag + 10%Magma	10%Opx + 80%Plag + 10%Magma
MgO	28.0	4.0	25.6	11.6	3.2
FeO	12.2	8.0	11.8	5.7	2.0
mg#	80.3	47.1	79.4	78.3	74
Rock Type			Pyroxenite	Norite	Anorthosite

The results obtained by Naldrett *et al.* (1986) and in this study are shown in Figures 13 to 15. In all of these diagrams it can be seen that the data plot along the general trends predicted by the curves calculated in Figure 12. In Figure 13 the data of Naldrett *et al.* (1986) show that the actual pyroxene compositions straddle curve C, determined in Figure 12. Thus the variation in En content in pyroxene and the correlation between En content and whole-rock MgO for the entire UG2 cyclic unit can be attributed entirely to the trapped liquid shift effect. Data from both mines appear indistinguishable. However, the pyroxene-rich samples (i.e. high MgO) from the Merensky Reef unit generally plot at lower En contents than the samples in the footwall. Exactly the same interpretations emerge for the data presented in Figure 14, taken from a single vertical section from this study.

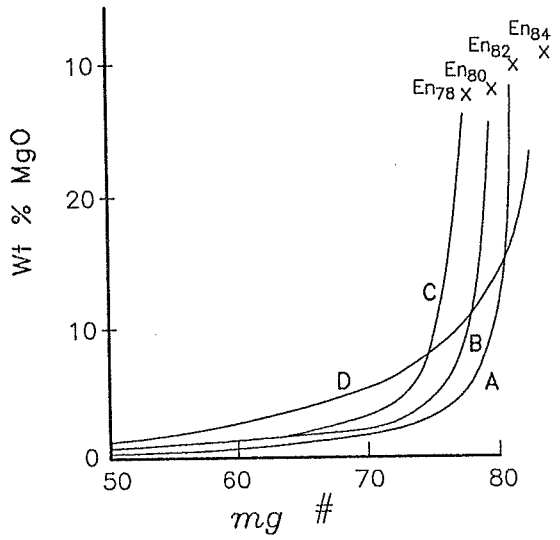

Figure 12: Calculated curves showing the whole-rock MgO and mg# compositions based on the trapped liquid shift model of Barnes (1986a). The curves A, B and C describe the change in bulk composition for primary pyroxenes with compositions En_{82}, En_{80} and En_{78} respectively, with a constant proportion of 10% trapped liquid. As the ratio of primary pyroxene to plagioclase decreases, both MgO and mg# decrease with a hyperbolic relationship. For curve D, 30% trapped liquid and a primary pyroxene composition of En_{84} are assumed.

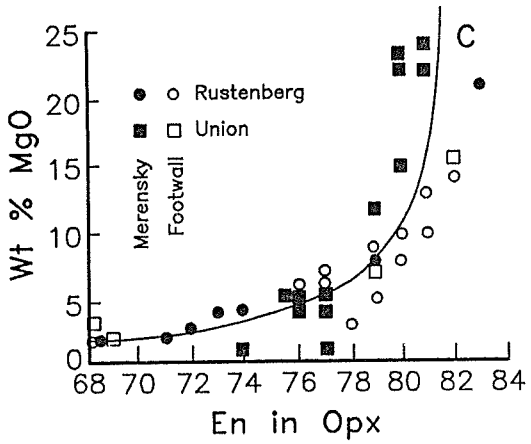

Figure 13: Plot of En content in pyroxene versus whole-rock MgO content from data of Naldrett et al. (1986). The curve C is taken from Figure 12. There is good agreement between the data and the model curve. Samples from the Merensky unit (filled symbols) generally have lower En contents than footwall samples (open symbols).

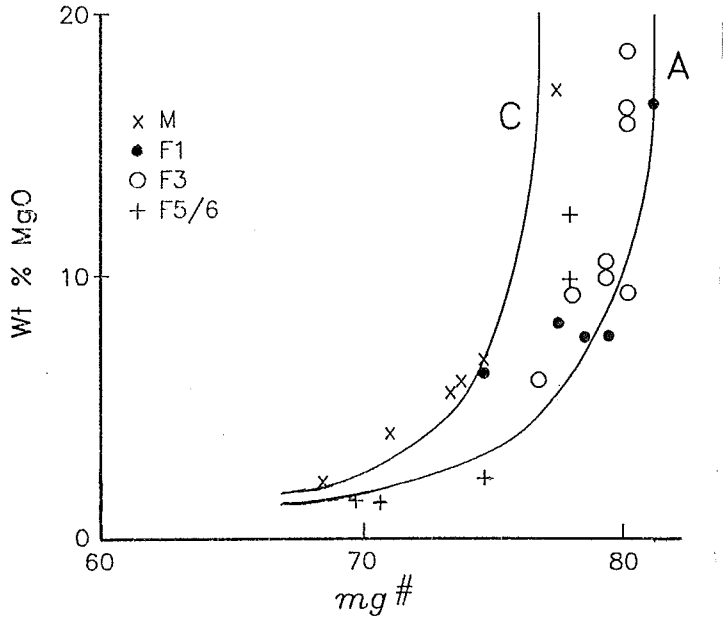

Figure 14: Plot of mg# value versus whole-rock MgO content for a single vertical borehole intersection. Curves A and C are the same curves as calculated in Figure 12. Samples from the Merensky unit (M), shown by crosses, plot at lower mg# values than footwall samples (F).

Figure 15 is a composite of all sections studied here, and includes 202 analyses. Curve B from Figure 12 is used as a discriminant. Of 95 analyses from the Merensky Reef unit, all but 8 plot on the low *mg#* side of this curve, whereas of the 107 footwall analyses all but 10 plot to the high *mg#* side. Hence, it can be concluded that there is a distinct difference in primary pyroxene composition between footwall and Merensky units, and that the Merensky unit has the lower *mg#* value.

The shape and position of the various actual curves defined by the data can be compared with modelled curves in Figure 12 to indicate both the composition of the primary pyroxene and the proportion of trapped liquid. Footwall samples in Fig. 14 define a curve similar to curve A in Figure 12, and hence indicate that the primary pyroxene at that level had a composition En_{82}. From this it is concluded that the magma from which the pyroxene crystallized contained 5-6% MgO (Fig. 8). The data from the Merensky unit define a curve similar to curve C in Figure 12, and so project back to a primary pyroxene composition of En_{80}, indicating a magma with only 4-5 per cent MgO.

Vertical sections where the modal proportion of pyroxene is constant have uniform pyroxene composition or constant whole-rock *mg#*, even over thick sequences (Fig. 10). Where modal pyroxene decreases upwards, so does the apparent En (or whole-rock *mg#*) content, even over very short vertical sections (M1 in Fig. 5). An upwards increase in

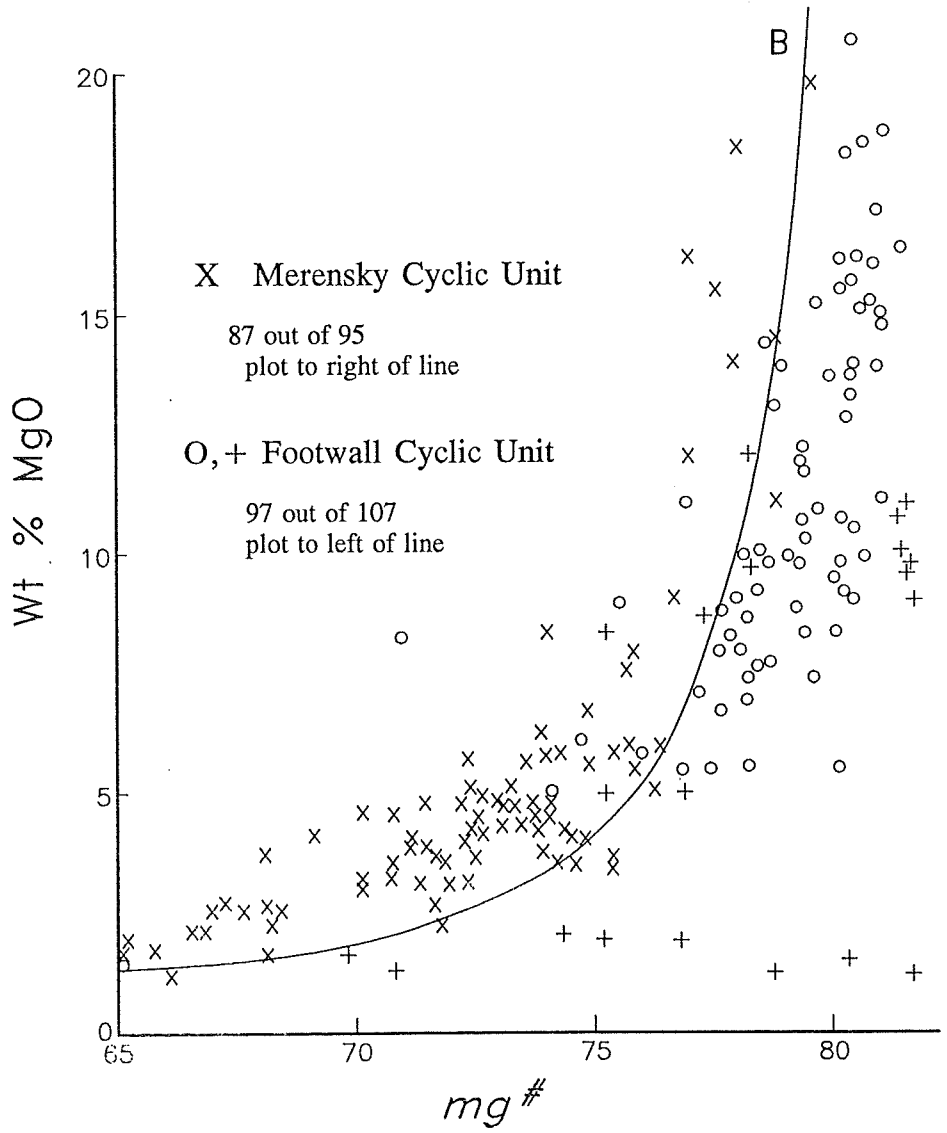

Figure 15: Plot of mg# value versus whole-rock MgO content for all twelve borehole intersections, totalling 202 samples. Sample designation as in Figure 14. Curve B is taken from Figure 12.

pyroxene content correlates with an increase in En or *mg#* (F3 in Fig. 11). Extremely sharp breaks in En or *mg#* value simply reflect equally sudden changes in mode (between F7 and F6 in Fig. 11). All these features are predicted by the trapped liquid shift effect. There is no need to appeal to complicated and frequent sequences of magma input and mixing, and variable amounts of fractionation over very short vertical intervals.

Migration of Sulphide Liquid

The ideal tracer for identifying migration of residual liquid would be one which was chemically very distinct, had a high density contrast with the surrounding cumulates and interstitial magma, had low viscosity, and only crystallized at temperatures below the solidus

of the silicate cumulates. Such a tracer exists, namely the sulphide liquid which formed at the base of the Merensky Reef. Its high Cu content makes it chemically distinct. It has a very high density and low viscosity in relation to its surroundings. It separated as an immiscible liquid at magmatic temperatures, but even at temperatures down to 1000°C the data of Fleet *et al.* (1993) show that it will only be about 50% crystallized. The sulphide occurs primarily in the pyroxenite of the Merensky Reef, but on Impala Platinum Mines is also present in the footwall. The extent of this can be seen by a plot of Cu content versus depth below the Merensky Reef in Figure 16. Immediately beneath normal Reef Cu contents reach over 1000 ppm, decreasing to values of less than 50 ppm within less than 5m. At greater depth, values remain at less than 50 ppm, which is typical of the entire footwall unit down to the UG2 chromitite (Schurmann, 1993). Assuming that this sulphide liquid separated at the same time as the Merensky Reef, these results indicate that the sulphide sank less than 5m into the crystal pile. As listed above, the physical properties of this sulphide liquid are such that they should be capable of migrating through interstitial space far more effectively than a silicate magma. The implication is that the latter would have migrated only extremely short distances.

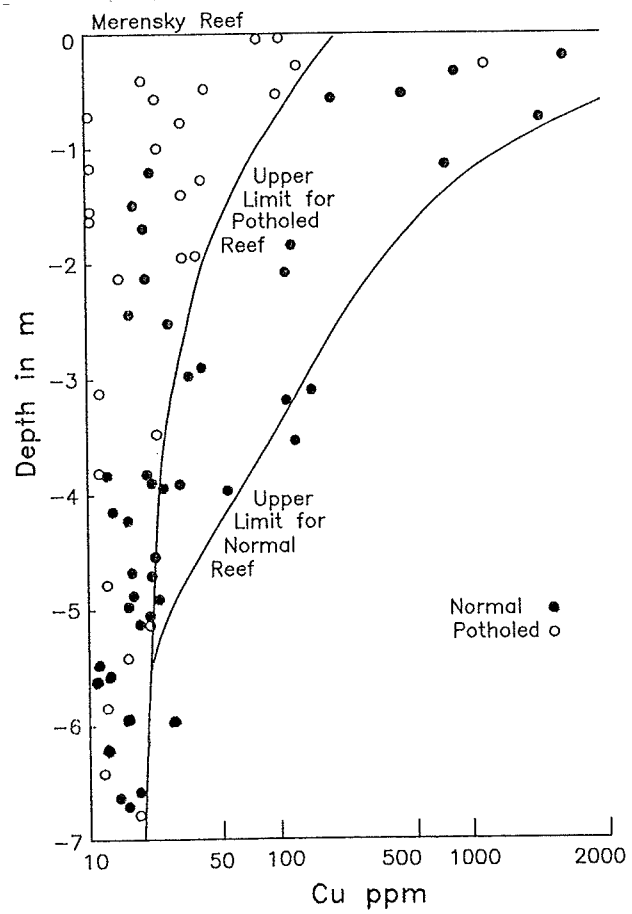

Figure 16: Plot of Cu content versus depth below the Merensky Reef for samples taken from ten boreholes. A log scale is used for the Cu content. Samples from potholed and normal Reef are distinguished. The curves indicate the upper limits of Cu for the two settings.

Of significance in Figure 16 is the fact that the footwall of potholed Reef shows enrichment in Cu of only a factor of two, and only over about 2m, relative to its deeper footwall. In the present study only profiles intersecting potholes which bottom against footwall 3 have been analyzed. Models for pothole formation can be divided into two. In one they are thought to have originated at the site of upwelling fluid or residual liquid (Boudreau, 1992). If they were the channelways for such processes they might be expected to contain higher proportions of interstitial magma and so be preferentially permeable compared to normal profiles. Such a situation would lead to greater, not lower, Cu contents in the footwall to potholes as observed in Figure 16.

The second general model for the formation of potholes attributes them to the physical removal of the immediate footwall layers either by mechanical or thermal mechanisms (Campbell, 1986). If this has occurred it is reasonable to assume that footwall 3 would have been more consolidated than footwall 1 at the time the pothole developed. At the time that the Merensky Reef and its sulphide began to accumulate the footwall 1 would have had higher permeability than the re-exhumed footwall 3 at the base of the pothole. The lack of enrichment of Cu below potholes in Figure 16 suggests that sulphide was unable to penetrate into footwall 3. It must therefore have been impermeable even to a sulphide liquid and so must have had almost zero porosity, even though it was less than 10m below the original magma-cumulate interface. Such adcumulates may form very close to this boundary by textural annealing, as demonstrated by Walker *et al.* (1988), rather than by infiltration of liquid through great thicknesses of crystal mush.

Proportion of Interstitial Magma

The shapes of the actual data curves in Figures 13 and 14 are more similar to the calculated curves for 10% rather than 30% trapped liquid (c.f. Fig. 12), and so indicate relatively low interstitial liquid content. These diagrams are interpreted to imply that all the rocks from the footwall sequence contained the same primary pyroxene composition, and the same proportion of trapped liquid and varied only in their plagioclase to pyroxene ratio. If this is correct it should be possible to take every whole-rock analysis, subtract the fixed proportion of magma (10 %), and determine the primary *mg#* or En content of the pyroxene. The MgO and FeO contents of the magma used in this calculation are taken from Table 2. This has been done in Figure 17, for the data presented in Figure 5. A remarkably uniform *mg#* value is obtained for the entire footwall sequence. In Figure 5B the *mg#* value in footwaal 1 to 6 varies from 70 to 83, whereas in Figure 17 this reduces to 79 to 84. Had the proportion of trapped magma been highly variable greater variability of *mg#* values would have resulted in Figure 17. Had the proportion of trapped liquid been higher, this calculation would have resulted in unrealistically high *mg#* values for leucocratic rocks. Had there been a lower proportion this would have resulted in leucocratic rocks still having anomalously low *mg#* values as seen in the raw data (Fig. 5B).

Determination of the trapped liquid content on the degree of curvature in diagrams such as Figures 13 and 14 is not reliable without other evidence. Trapped liquid content can also be estimated using the abundances of incompatible elements. The whole-rock content of Zr and K_2O have therefore also been used to estimate the trapped liquid content. In order to do this it is necessary to infer a concentration for these elements in the magma. Values of

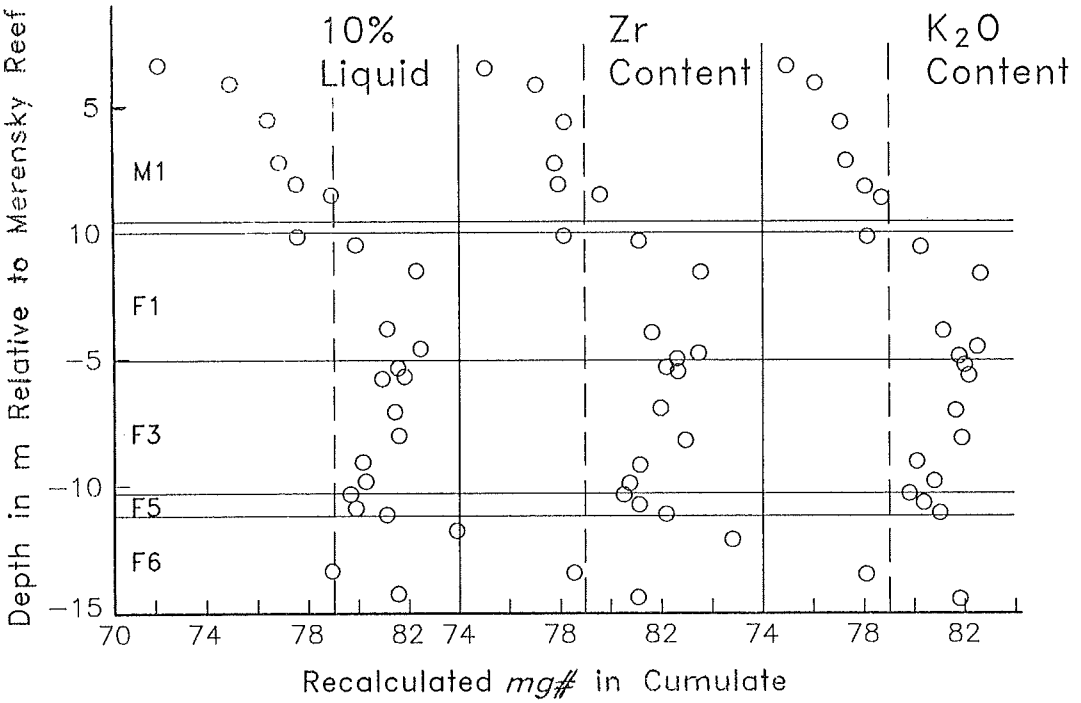

Figure 17: Plot of recalculated whole-rock mg# value versus depth relative to the Merensky Reef. In the first column a uniform 10% trapped liquid in all samples has been assumed, removed from the whole-rock analysis and the primary mg# value determined. In the next two columns the proportion of trapped liquid has been calculated from the abundance of Zr and K_2O, respectively, and again subtracted from whole-rock composition to give primary mg# values.

150 ppm Zr and 1.5 per cent K_2O have been used. These are double the values determined for the parental magma to the Bushveld Complex, as 50 per cent fractionation has been inferred from the experimental studies reported in Figure 8. The proportion of interstitial liquid calculated in this way is given in Table 1. Using these two parameters, primary *mg#* values have been calculated in Figure 17, and show extremely good agreement with those using a constant value of 10%, suggesting that this is a reasonable estimate for this suite of rocks.

The two methods (curve-fitting and incompatible element contents) of calculating primary *mg#* values for the Merensky unit do not indicate a uniform primary pyroxene composition (Fig. 17), but suggest that rapid differentiation or mixing with more evolved magma is taking place during the formation of this interval.

CONCLUSIONS

The rock sequence from the Upper Group 2 Chromitite to the Merensky Reef is not a simple cyclic unit. It contains 13 distinct layers with variable proportions of plagioclase to pyroxene. Similarly, the trend of *mg#* content in pyroxene and whole rock is not smooth. Forward and reverse breaks may occur over very short vertical intervals, but variations always correlate with modal abundance of pyroxene. Reversals occur where modal pyroxene

increases, and forward breaks where pyroxene decreases. Such observations are difficult to explain if these compositions are taken to reflect primary mineral compositions. However, they are totally predictable if a constant primary pyroxene composition of En_{82} is assumed and observed variations are related to the trapped liquid shift effect. Two independent techniques for estimating the proportion of trapped liquid yield values of about 10%. The entire UG2 cyclic unit, which is over 100m formed from a magma of a constant composition, whereas in 20m of the overlying Merensky Reef unit there is evidence of considerable differentiation.

Contrary to many previous assumptions it is shown that the Merensky Reef and its footwall did not form from ultrabasic magma, but from magmas with 4-6% MgO. Furthermore, the Merensky Reef magma was more evolved than the footwall magma.

The only evidence for migration of liquid that can be identified is of immiscible sulphide liquid. This has migrated less than 5m into the footwall of the Merensky Reef despite its very high density contrast with silicate magma, low viscosity and low crystallization temperature, all of which should facilitate infiltration.

These observations probably relate to the extremely slow cooling rate of this enormous intrusion. They may not apply in shallow-level and small bodies.

ACKNOWLEDGEMENTS

Access to bore core samples, courtesy of Genmin and Impala Platinum Mines, and their permission to publish these results, are gratefully acknowledged. I thank my wife Patricia and Ms S Hall for crushing and analyzing samples, and Ms L Whitfield and D du Toit for preparing diagrams. Financial assistance was provided by the Foundation for Research Development (South Africa).

REFERENCES

Barnes, S.J. (1986a). The effect of trapped liquid crystallization on cumulus mineral compositions in layered intrusions. *Contrib. Mineral. Petrol.*, **93**, 524-531.

Barnes, S.J. (1986b). The distribution of chromium among orthopyroxene, spinel and silicate liquid at atmospheric pressure. *Geochim. Cosmochim. Acta*, **50**, 1889-1909.

Boudreau, A.E. (1992). Volatile fluid overpressure in layered intrusions and the formation of potholes. *Austral. J. Earth Sci.*, **39**, 277-287.

Boudreau, A.E. and McCallum, I.S. (1992). Concentration of platinum-group elements by magmatic fluids in layered intrusions. *Econ. Geol.*, **87**, 1830-1848.

Campbell, I.H. (1986). A fluid dynamic model for the potholes of the Merensky Reef. *Econ. Geol.*, **81**, 1118-1125.

Cawthorn, R.G. and Biggar, G.M. (1993). Crystallization of titaniferous chromite, magnesian ilmenite and armalcolite in tholeiitic suites in the Karoo Igneous Province. *Contrib. Mineral. Petrol.*, **114**, 221-235.

Cawthorn, R.G. and Davies, G. (1983). Experimental data at 3 kbars pressure on parental magma to the Bushveld Complex. *Contrib. Mineral. Petrol.*, **52**, 81-89.

Cawthorn, R.G. and Poulton, K.L. (1988). Evidence for fluid in the footwall beneath potholes in the Merensky Reef of the Bushveld Complex. *In: Geo-platinum 87.* Pritchard, H.M., Potts, P.J., Bowles, J.F.W. and Cribb, S.J. (eds.). Elsevier, London, 343-356.

Eales, H.V., Botha, W.J., Hattingh, P.J., De Klerk, W.J., Maier, W.D. and Odgers, A.T. (1993). The mafic rocks of the Bushveld Complex: a review of emplacement and crystallization histroy, and mineralization, in the light of new data. *J. Afr. Earth Sci.*, **16,** 121-142.

Eales, H.V., Field, M., De Klerk, W.J. and Scoon, R. (1988). Regional trends of chemical variation and thermal erosion in the upper Critical Zone, western Bushveld Complex. *Mineral. Mag.*, **52**, 63-79.

Eales, H.V., Marsh, J.S., Mitchell, A.A., De Klerk, W.J., Kruger, F.J. and Field, M. (1986). Some geochemical constraints upon models for the crystallization of the upper Critical Zone - Main Zone interval, northwestern Bushveld Complex. *Mineral. Mag.*, **50**, 567-582.

Eales, H.V., Teigler, B. and Maier, W.D. (1993). Cryptic variations of minor elements Al, Cr, and Mn in Lower and Critical Zone orthopyroxenes of the western Bushveld Complex. *Mineral. Mag.*, **57**, 257-264.

Fleet, M.E., Chryssoulis, S.L., Stone, W.E. and Weisener, C.G. (1993). Partitioning of platinum-group elements and Au in the Fe-Ni-Cu-S system: experiments on the fractional crystallization of sulphide melt. *Contrib. Mineral. Petrol.*, **115**, 36-44.

Ferguson, J. (1969). Compositional variation in minerals from mafic rocks of the Bushveld Complex. *Trans. Geol. Soc. S. Afr.*,**72**, 61-78.

Harmer, R.E. and Sharpe, M.R. (1985). Field relations and strontium isotope systematics of the marginal rocks of the eastern Bushveld Complex. *Econ. Geol.*, **80**, 813-837.

Irvine, T.N. (1980). Magmatic infiltration metasomatism, double-diffusive fractional crystallization, and adcumulus growth in the Muskox intrusion and other layered intrusions. *In: Physics of Magmatic Processes.* Hargraves, R.B. (ed.)., Princeton University Press, Princeton, New Jersey, 326-383.

Irvine, T.N., Keith, D.W. and Todd, S.G. (1983). The J-M platinum-palladium reef of the Stillwater Complex, Montana. II. Origin by double-diffusive convective magma mixing and implications for the Bushveld Complex. *Econ. Geol.* , **78**, 1287-1334.

Kruger, F.J. and Marsh, J.S. (1982). Significance of $^{87}Sr/^{86}Sr$ ratios in the Merensky Cyclic Unit of the Bushveld Complex. *Nature*, **298**, 53-55.

Leeb-du Toit, A. (1986). The Impala platinum mines. *In: Mineral Deposits of Southern Africa, vol. 2.* Anhaeusser, C.R. and Maske, S. (eds.). Geol. Soc. S. Afr., Johannesburg, 1091-1106.

McKenzie, D.P. (1984). The generation and compaction of partially molten rock. *J. Petrol.*, **25**, 713-765.

Naldrett, A.J., Gasparrini, E.C., Barnes, S.J., Von Gruenewaldt, G. and Sharpe, M.R. (1986). The upper Critical Zone of the Bushveld Complex and a model for the origin of Merensky-type ores. *Econ. Geol.*, **81**, 1105-1118.

Robins, B. (1982). Finger structures in the Lille Kufjord layered intrusion, Finmark, northern Norway. *Contrib. Mineral. Petrol.*, **81**, 290-295.

Schurmann, L.W. (1993). The geochemistry and petrology of the upper Critical Zone of the Boshoek section of the western Bushveld Complex. *Geol. Surv. S. Afr. Bull.*, **113**, 88pp.

Tait, S.R. and Jaupart, C. (1992). Compositional convection in a reactive crystalline mush and melt differentiation. *J. Geophys. Res.*, **97**, 6735-6756.

Tait, S.R., Huppert, H.E. and Sparks, R.S.J. (1984). The role of compositional convection in the formation of adcumulate rocks. *Lithos*, **17**, 139-146.

Wager, L.R., Brown, G.M. and Wadsworth, W.J. (1960). Types of igneous cumulates. *J. Petrol.*, **1**, 73-85.

Walker, D., Jurewitz, S. and Watson, E.B. (1988). Adcumulus growth in a laboratory thermal gradient. *Contrib. Mineral. Petrol.*, **99**, 306-319.

_____oOo_____